TWMS J. Pure Appl. Math. V.12, N.2, 2021, pp.223-242

DYNAMICS OF THE MOVING RING-LOAD ACTING IN THE INTERIOR OF THE BI-LAYERED HOLLOW CYLINDER WITH IMPERFECT CONTACT BETWEEN THE LAYERS

S.D. AKBAROV[1,2], M.A. MEHDIYEV[2], A.M. ZEYNALOV[3]

Abstract. The dynamics of the moving-with-constant-velocity internal ring-load (-pressure) acting on the inner surface of the bi-layered hollow circular cylinder is studied within the scope of the piecewise homogeneous body model by employing the exact field equations of the linear theory of elastodynamics. It is assumed that the internal pressure is point-located with respect to the cylinder axis and is axisymmetric in the circumferential direction. Moreover, it is assumed that shear-spring type imperfect contact conditions on the interface between the layers of the cylinder are satisfied. The focus is on determination of the critical velocity with analyses of the interface stress distribution and their attenuation rules with respect to time. At the same time, there is analysis of the problem parameters such as the ratio of modulus of elasticity, the ratio of the cylinder's layers thickness to the external radius of inner layer-cylinder, and the shear-spring type parameter which characterizes the degree of the contact imperfection on the values of the critical velocity and stress distribution. Corresponding numerical results are presented and discussed. In particular, it is established that the values of the critical velocity of the moving ring-load increase with the thickness of the external layer of the cylinder.

Keywords: moving ring-load, critical velocity, bi-layered hollow cylinder, shear-spring type imperfection, interface stresses.

AMS Subject Classification: 74F10.

1. Introduction

A cannon bullet has its initial velocity through the moving in the interior of the cannon which in many cases can be modelled as a circular hollow cylinder. The moving of the bullet accompanied by a certain internal pressure which can be modelled as a moving axisymmetric ring-load. In order to control the safety and to modernize of the cannons it is necessary to study and to know the patterns of the dynamics of the aforementioned moving internal pressure. As the main issue in the investigations related to the moving load is to determination of the critical velocity of the moving load under which the resonance type accident takes place, therefore the aforementioned studies must be focused on the determination of this critical velocity and on the influence of the problem parameters on this velocity. In the sense of the modernization of cannons, for instance, it is interesting to know how the use of the bi-layered cylinder instead of the homogeneous hollow cylinder can act on the values of the critical velocity of the moving internal pressure and how it can be controlled the values of this critical velocity through the mechanical and geometrical parameters of the additional external hollow cylinder. Namely, the study of these and other related questions is the subject of the present paper.

[1]Department of Mechanical Engineering, Yildiz Technical University, Istanbul, Turkey
[2]Azerbaijan State University of Economics, Baku, Azerbaijan
[3]Ganja State University, Ganja, Azerbaijan
e-mail: akbarov@yildiz.edu.tr, mahirmehdiyev@mail.ru
Manuscript received April 2019.

To determine the significance and place of the present investigations among the other related ones we consider a brief review of those and note that the first attempt in this field was made by Achenbach et al. [2] in which the dynamic response of the system consisting of the covering layer and half plane to a moving load was investigated with the use of the Timoshenko theory for describing the motion of the plate. However, the motion of the half-plane was described by using the exact equations of the theory of linear elastodynamics and the plane-strain state was considered. It was established that critical velocity exists in the cases where the plate material is stiffer than that of the half-plane material. Reviews of later investigations, which can be taken as developments of those started in the paper [2], are described in the papers [21, 28]. At the same time, in the paper [21] the critical velocity of a point-located time-harmonic varying and unidirectional moving load which acts on the free face plane of the plate resting on the rigid foundation, was investigated. The investigations were made within the scope of the 3D exact equations of the linear theory of elastodynamics and it was established that as a result of the time-harmonic variation of the moving load, two types of critical velocities appear: the first (the second) of which is lower (higher) than the Rayleigh wave velocity in the plate material. Later, similar results were also obtained in the papers [7-10], which were also discussed in the monograph [5]

Note that up to now, a certain number of investigations have also been made related to the dynamics of the moving load acting on the pre-stressed system. For instance, in the paper [27], the initial stresses on the values of the critical velocity of the moving load acting on an ice plate resting on water were taken into account. In this paper, the motion of the plate is described by employing the Kirchhoff plate theory and it is established that the initial stretching (compression) of the plate along the load moving direction causes an increase (a decrease) in the values of the critical velocity.

The paper [28] deals with the investigation of the lateral vibration of the beam on an elastic half-space due to a moving lateral time-harmonic load acting on the beam, the initial axial compression of this beam is also taken into consideration. In this investigation, the motion of the beam is written through the Euler-Bernoulli beam theory, however, the motion of the half-space is described by the 3D exact equations of elastodynamics and it is assumed there are no initial stresses in the half-space.

Moreover, the influence of the initial stresses acting in the half-plane on the critical velocity of the moving load which acts on the plate which covers this half-plane was studied in the papers [16-19] in which the plane strain state was considered and the motion of the half-plane was written within the scope of the three-dimensional linearized theory of elastic waves in initially stressed bodies. However, the motion of the covering layer, which does not have any initial stresses, as in the paper [2], was written by employing the Timoshenko plate theory and the plane-strain state is considered.

Moreover, in the paper [6], the influence of the initial stresses in the covering layer and half-plane on the critical velocity of the moving load acting on the plate covering the half-plane, was studied. The same moving load problem for the system consisting of the covering layer, substrate and half-plane was studied in the paper [22]. The dynamics of the system consisting of the orthotropic covering layer and orthotropic half plane under action of the moving and oscillating moving load were investigated in the papers [8, 9] and the influence of the initial stresses in the constituents of this system on the values of the critical velocity was examined in the paper [24].

Finally, we note the paper [11] in which the dynamics of the lineally-located moving load acting on the hydro-elastic system consisting of elastic plate, compressible viscous fluid and rigid wall were studied. It was established that there exist cases under which the critical velocities appear.

Note that related non-linear problems regarding the moving and interaction of two solitary waves was examined in the paper [20] and other ones cited therein. At the same time, non-stationary dynamic problems for viscoelastic and elastic mediums were studied in the papers [25, 3] and other works cited in these papers. Moreover, it should be noted that up to now it has been made considerable number investigations on fluid flow-moving around the stagnation-point (see the paper [14] and other works listed therein). Some problems related to the effects of magnetic field and the free stream flow-moving of incompressible viscous fluid passing through magnetized vertical plate were studied in [16].

The investigations related to the fluid-plate and fluid-moving plate interaction were considered the papers [12, 13].

It follows from the foregoing brief review that almost all investigations on the dynamics of the moving and oscillating moving load relate to flat-layered systems. However, as noted in the beginning of this section, cases often occur in practice in which it is necessary to apply a model consisting of cylindrical layered systems, one of which is the hollow cylinder surrounded by an infinite or finite deformable medium under investigation of the dynamics of a moving or oscillating moving load. It should be noted that up to now some investigations have already been made in this field. For instance, in the paper by Abdulkadirov [1] and others listed therein, the low-frequency resonance axisymmetric longitudinal waves in a cylindrical layer surrounded by an infinite elastic medium were investigated. Note that under "resonance waves" the cases under which the relation $dc/dk = 0$ occurs, is understood, where c is the wave propagation velocity and k is the wavenumber. It is evident that the velocity of these "resonance waves" is the critical velocity of the corresponding moving load. Some numerical examples of "resonance waves" are presented and discussed. It should be noted that in the paper [1], in obtaining dispersion curves, the motion of the hollow cylinder and surrounding elastic medium is described through the exact equations of elastodynamics, however, under investigation of the displacements and strains in the hollow cylinder under the wave process, the motion of the hollow cylinder is described by the classical Kirchhoff-Love theory.

Another example of the investigations related to the problems of the moving load acting on the cylindrical layered system is the investigation carried out in the paper [33] in which the critical velocity of the moving internal pressure acting in the sandwich shell was studied. Under this investigation, two types of approaches were used, the first of which is based on first order refined sandwich shell theories, while the second approach is based on the exact equations of linear elastodynamics for orthotropic bodies with effective mechanical constants, the values of which are determined by the well-known expressions through the values of the mechanical constants and volumetric fraction of each layer of the sandwich shell. Numerical results on the critical velocity obtained within these approaches are presented and discussed. Comparison of the corresponding results obtained by these approaches shows that they are sufficiently close to each other for the low wavenumber cases, however, the difference between these results increases with the wavenumber and becomes so great that it appears necessary to determine which approach is more accurate. It is evident that for this determination it is necessary to investigate these problems by employing the exact field equations of elastodynamics within the scope of the piecewise homogeneous body model, which is also used in the present paper. The other drawback of the approach used in the paper [33] is the impossibility to calculation of the interface stresses between the cylinder's layers with enough accuracy. It is evident that such calculation of the

interface stresses from which depends directly the adhesion strength of the layered cylinder, must be also made within the scope of the piece-wise homogeneous body model with employing the exact equations and relations of the elastodynamics.

Taking the foregoing statements into account, in the present paper we attempt to investigate the dynamics of the moving ring load in the interior of the bi-layered hollow cylinder within the scope of the piecewise homogeneous body model with the use of the exact equations and relations of the elastodynamics. During this investigation the main attention is focused not only on the critical velocity of the moving load and on the influence of the problem parameters on this velocity, but also on the interface stresses appearing as a result of the mentioned moving load.

2. Mathematical formulation of the problem

Consider a bi-layered hollow circular cylinder with internal (external) layer thickness h_2 (h_1) (Fig.1). We associate the cylindrical and Cartesian systems of coordinates $Or\theta z$ and $Ox_1x_2x_3$ (Fig. 1) with the central axis of this cylinder. Assume that the external radius of the cross section of the inner layer-cylinder is R and on its inner surface axisymmetric uniformly distributed normal ring-forces moving with constant velocity V act and these forces are point-located with respect to the cylinder central axis. Within this framework, we investigate the axisymmetric stress-strain state in this bi-layered cylinder by employing the exact equations of the linear theory of elastodynamics within the scope of the piecewise homogeneous body model. Below, the values related to the inner and to the outer layer will be denoted by upper indices (2) and (1), respectively.

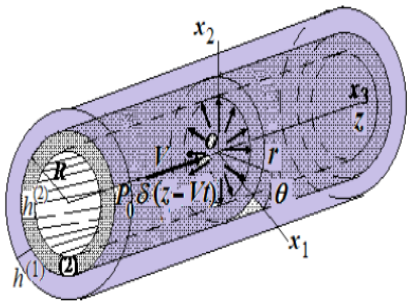

Figure 1. The geometry of the system under consideration.

We suppose that the materials of the constituents are homogeneous and isotropic. We write the field equations and contact conditions as follows.

Equations of motion:

$$\frac{\partial \sigma_{rr}^{(k)}}{\partial r}+\frac{\partial \sigma_{rz}^{(k)}}{\partial z}+\frac{1}{r}(\sigma_{rr}^{(k)}-\sigma_{\theta\theta}^{(k)})=\rho^{(k)}\frac{\partial^2 u_r^{(k)}}{\partial t^2},$$

$$\frac{\partial \sigma_{rz}^{(k)}}{\partial r}+\frac{\partial \sigma_{zz}^{(k)}}{\partial z}+\frac{1}{r}\sigma_{rz}^{(k)}=\rho^{(k)}\frac{\partial^2 u_z^{(k)}}{\partial t^2}. \tag{1}$$

Elasticity relations:

$$\sigma_{nn}^{(k)}=\lambda^{(k)}(\varepsilon_{rr}^{(k)}+\varepsilon_{\theta\theta}^{(k)}+\varepsilon_{zz}^{(k)})+2\mu^{(k)}\varepsilon_{nn}^{(k)}, nn=rr;\ \theta\theta;\ zz, \sigma_{rz}^{(k)}=2\mu^{(k)}\varepsilon_{rz}^{(k)}. \tag{2}$$

Strain – displacement relations:

$$\varepsilon_{rr}^{(k)} = \frac{\partial u_r^{(k)}}{\partial r}, \varepsilon_{\theta\theta}^{(k)} = \frac{u_r^{(k)}}{r}, \varepsilon_{zz}^{(k)} = \frac{\partial u_z^{(k)}}{\partial z}, \varepsilon_{rz}^{(k)} = \frac{1}{2}(\frac{\partial u_z^{(k)}}{\partial r} + \frac{\partial u_r^{(k)}}{\partial z}). \tag{3}$$

Note that the equations (1), (2) and (3) are the complete system of the field equations of the linear theory of elastodynamics in the case under consideration and in these equations conventional notation is used.

Consider the formulation of the boundary and contact conditions. According to the foregoing description of the problem, the boundary conditions on the inner face surface of the inner leyer-cylinder can be formulated as follows.

$$\sigma_{rr}^{(2)}\Big|_{r=R-h_2} = -P_0\delta(z-Vt), \sigma_{rz}^{(2)}\Big|_{r=R-h_2} = 0. \tag{4}$$

We assume that the contact conditions with respect to the forces and radial displacement are continuous and can be written as follows:

$$\sigma_{rr}^{(1)}\Big|_{r=R} = \sigma_{rr}^{(2)}\Big|_{r=R}, \sigma_{rz}^{(1)}\Big|_{r=R} = \sigma_{rz}^{(2)}\Big|_{r=R}, u_r^{(1)}\Big|_{r=R} = u_r^{(2)}\Big|_{r=R}. \tag{5}$$

At the same time, we assume that shear-spring type imperfection occurs in the contact condition related to the axial displacements and, according to [5] and others listed therein, this condition is formulated by the following equation:

$$u_z^{(1)}\Big|_{r=R} - u_z^{(2)}\Big|_{r=R} = \frac{FR}{\mu^{(1)}}\,\sigma_{rz}^{(1)}\Big|_{r=R}. \tag{6}$$

The dimensionless parameter F in (6) characterizes the degree of the imperfection and the range of change of this parameter is $-\infty \le F \le \infty$. Note that the case where $F = 0$ corresponds to complete contact, but the cases where $F = \pm\infty$ correspond to full slipping contact conditions.

Moreover, we assume that on the external surface of the external layer-cylinder the following boundary conditions are satisfied.

$$\sigma_{rr}^{(1)}\Big|_{r=R+h_1} = 0, \sigma_{rz}^{(1)}\Big|_{r=R+h_1} = 0. \tag{7}$$

We also suppose that

$$V < \min\left\{c_2^{(1)}; c_2^{(2)}\right\}, c_2^{(n)} = \sqrt{\mu^{(n)}\Big/\rho^{(n)}}, n = 1, 2, \tag{8}$$

i.e. we will consider the subsonic moving velocity.

This completes formulation of the problem and consideration of the governing field equations.

3. Method of solution

In general, for the solution of the problems related to mathematical physics, it is applied various numerical and analytical-numerical methods some of which are detailed in the papers [13, 29 - 31]. According to this classification of the solution methods, in the present paper, we employ the analytical-numerical method and for solution to the problem formulated above the well-known, classical Lame (or Helmholtz) decomposition (see, for instance, Eringen and Suhubi [23]) is used:

$$u_r^{(k)} = \frac{\partial \Phi^{(k)}}{\partial r} + \frac{\partial^2 \Psi^{(k)}}{\partial r \partial z}, u_z^{(k)} = \frac{\partial \Phi^{(k)}}{\partial z} + \frac{\partial^2 \Psi^{(k)}}{\partial z^2} - \frac{1}{(c_2^{(k)})^2}\frac{\partial^2 \Psi^{(k)}}{\partial t^2}, \tag{9}$$

where $\Phi^{(k)}$ and $\Psi^{(k)}$ satisfy the following equations:

$$\nabla^2\Phi^{(k)} - \frac{1}{(c_1^{(k)})^2}\frac{\partial^2\Phi^{(k)}}{\partial t^2} = 0\,, \nabla^2\Psi^{(k)} - \frac{1}{(c_2^{(k)})^2}\frac{\partial^2\Psi^{(k)}}{\partial t^2} = 0, \nabla^2 = \frac{\partial^2}{\partial r^2} + \frac{1}{r}\frac{\partial}{\partial r} + \frac{\partial^2}{\partial z^2}, \tag{10}$$

where $c_1^{(k)} = \sqrt{(\lambda^{(k)} + \mu^{(k)})/\rho^{(k)}}$ and $c_2^{(k)} = \sqrt{\mu^{(k)}/\rho^{(k)}}$.

We use the moving coordinate system

$$r' = r, z' = z - Vt \tag{11}$$

which moves with the loading internal pressure and by rewriting the Eq. (10) with the coordinates r' and z', we obtain:

$$\nabla^2\Phi^{(k)} - \frac{V^2}{(c_1^{(k)})^2}\frac{\partial^2\Phi^{(k)}}{\partial z^2} = 0\,, \nabla^2\Psi^{(k)} - \frac{V^2}{(c_2^{(k)})^2}\frac{\partial^2\Psi^{(k)}}{\partial z^2} = 0, \tag{12}$$

where the primes on the r and z have been omitted. After coordinate transformation (11) the first condition in (4) transforms to the following one:

$$\sigma_{rr}^{(2)}\Big|_{r=R-h_2} = -P_0\delta(z), \tag{13}$$

but the other relations and conditions in (1) – (8) remain valid in the new coordinates determined by (11).

Below we will use the dimensionless coordinates $\bar{r} = r/h_2$ and $\bar{z} = z/h_2$ instead of the coordinates r and z, respectively and the over-bar in $\bar{r}$ and $\bar{z}$ will be omitted.

Thus, the solution of the considered boundary value problem is reduced to the solution to the equations in (12). For this purpose we use the Fourier transformation with respect to the coordinate z and by taking the problem symmetry with respect to the point $z = 0$ into consideration, the functions $\Phi^{(k)}$, $\Psi^{(k)}$and the other sought values can be presented as follows.

$$\left\{\Phi^{(k)}; u_r^{(k)}; \sigma_{nn}^{(k)}; \varepsilon_{nn}^{(k)}\right\}(r,z) = \frac{1}{\pi}\int_0^\infty \left\{\Phi_F^{(k)}; u_{rF}^{(k)}; \sigma_{nnF}^{(k)}; \varepsilon_{nnF}^{(k)}\right\}(r,s)\cos(sz)ds, nn = rr;\ \theta\theta;\ zz$$

$$\left\{\Psi^{(k)}; u_z^{(k)}; \sigma_{rz}^{(k)}; \varepsilon_{rz}^{(k)};\right\}(r,z) = \frac{1}{\pi}\int_0^\infty \left\{\Psi_F^{(k)}; u_{zF}^{(k)}; \sigma_{rzF}^{(k)}; \varepsilon_{rzF}^{(k)}\right\}(r,s)\sin(sz)ds. \tag{14}$$

Substituting the expressions in (14) into the foregoing equations, relations and contact and boundary conditions, we obtain the corresponding ones for the Fourier transformations of the sought values. Note that after this substitution, the relation (2), the first and second relation in (3), the second condition in (4) and all the conditions in (5), (6) and (7) remain as for their Fourier transformations. However, the third and fourth relation in (3) and the condition (13) and the relations in (9) transform to the following ones:

$$\varepsilon_{zzF}^{(k)} = su_{zF}^{(k)}, \varepsilon_{rzF}^{(k)} = \frac{1}{2}(\frac{du_{zF}^{(k)}}{dr} + su_{rF}^{(k)}),\ \sigma_{rrF}^{(2)}\Big|_{r=R-h} = -P_0.$$

$$u_{rF}^{(k)} = \frac{d\Phi_F^{(k)}}{dr} + s\frac{d\Psi_F^{(k)}}{dr}, u_{zF}^{(k)} = -s\Phi_F^{(k)} - s^2(1 - \frac{V^2}{(c_2^{(k)})^2})\Psi_F^{(k)}. \tag{15}$$

Moreover, after the aforementioned substitution we obtain the following equations for $\Phi_F^{(k)}$ and $\Psi^{(k)}$ from the equations in (12).

$$\left[\frac{d^2}{dr^2}+\frac{1}{r}\frac{d}{dr}-s^2(1-\frac{V^2}{(c_1^{(k)})^2})\right]\Phi_F^{(k)}=0,\left[\frac{d^2}{dr^2}+\frac{1}{r}\frac{d}{dr}-s^2(1-\frac{V^2}{(c_2^{(k)})^2})\right]\Psi_F^{(k)}=0. \tag{16}$$

According to the condition (7), the solution to the equations in (16) we find as follows:

$$\Phi_F^{(2)}=A_1^{(2)}I_0(q_1^{(2)}r)+A_2^{(2)}K_0(q_1^{(2)}r),\Phi_F^{(1)}=A_1^{(1)}I_0(q_1^{(1)}r)+A_2^{(1)}K_0(q_1^{(1)}r),$$

$$\Psi_F^{(2)}=B_1^{(2)}I_0(q_2^{(2)}r)+B_2^{(2)}K_0(q_2^{(2)}r),\Psi_F^{(1)}=B_1^{(1)}I_0(q_2^{(1)}r)+B_2^{(1)}K_0(q_2^{(1)}r),$$

$$q_1^{(k)}=\sqrt{s^2(1-\frac{V^2}{(c_1^{(k)})^2})},q_2^{(k)}=\sqrt{s^2(1-\frac{V^2}{(c_2^{(k)})^2})}. \tag{17}$$

Here $I_0(x)$ and $K_0(x)$ are modified Bessel functions for the purely imaginary arguments of the first and second kind, respectively with zeroth order.

Thus, using the expressions (2), (3), (9), (15) and (17) we obtain the following expressions of the Fourier transformations of the sought values.

$$u_{rF}^{(k)}=A_1^{(k)}q_1^{(k)}I_1(q_1^{(k)}r)-A_2^{(k)}q_1^{(k)}K_1(q_1^{(k)}r)+B_1^{(k)}sq_2^{(k)}I_1(q_2^{(k)}r)-B_2^{(k)}sq_2^{(k)}K_1(q_2^{(k)}r),$$

$$u_{zF}^{(k)}=-A_1^{(k)}sI_0(q_1^{(k)}r)-A_2^{(k)}sK_0(q_1^{(k)}r)-B_1^{(k)}q_2^{(k)}I_0(q_1^{(k)}r)-B_2^{(k)}q_2^{(k)}K_0(q_1^{(k)}r),$$

$$\sigma_{rzF}^{(k)}=\mu^{(k)}\left[A_1^{(k)}\left(0.5(q_1^{(k)})^2(I_0(q_1^{(k)}r)+I_2(q_1^{(k)}r))-s^2I_0(q_1^{(k)}r)\right)+\right.$$
$$A_2^{(k)}\left(0.5(q_1^{(k)})^2(K_0(q_1^{(k)}r)+K_2(q_1^{(k)}r))-s^2K_0(q_1^{(k)}r)\right)+$$
$$B_1^{(k)}\left(0.5s(q_2^{(k)})^2(I_0(q_2^{(k)}r)+I_2(q_2^{(k)}r))-sq_2^{(k)}I_0(q_2^{(k)}r)\right)+$$
$$\left.B_2^{(k)}\left(0.5s(q_2^{(k)})^2(K_0(q_2^{(k)}r)+K_2(q_2^{(k)}r))-sq_2^{(k)}K_0(q_2^{(k)}r)\right)\right],$$

$$\sigma_{rrF}^{(k)}=2\mu^{(k)}\left[A_1^{(k)}\left[(1+\frac{\lambda^{(k)}}{2\mu^{(k)}})(q_1^{(k)})^20.5(I_0(q_1^{(k)}r)+I_2(q_1^{(k)}r))+\right.\right.$$
$$\left.\frac{\lambda^{(k)}}{2\mu^{(k)}}(\frac{q_1^{(k)}}{r}I_1(q_1^{(k)}r)-s^2I_0(q_1^{(k)}r))\right]+$$
$$A_2^{(k)}\left[(1+\frac{\lambda^{(k)}}{2\mu^{(k)}})(q_1^{(k)})^20.5(K_0(q_1^{(k)}r)+K_2(q_1^{(k)}r))+\right.$$
$$\left.\frac{\lambda^{(k)}}{2\mu^{(k)}}(-\frac{q_1^{(k)}}{r}K_1(q_1^{(k)}r)-s^2K_0(q_1^{(k)}r))\right]+$$
$$B_1^{(k)}\left[(1+\frac{\lambda^{(k)}}{2\mu^{(k)}})s(q_2^{(k)})^20.5(I_0(q_2^{(k)}r)+I_2(q_2^{(k)}r))\right.$$
$$\left.+\frac{\lambda^{(k)}}{2\mu^{(k)}}(\frac{sq_2^{(k)}}{r}I_1(q_2^{(k)}r)-sq_2^{(k)}I_0(q_2^{(k)}r))\right]+$$

$$B_2^{(k)}\left[(1+\frac{\lambda^{(k)}}{2\mu^{(k)}})s(q_2^{(k)})^2 0.5(K_0(q_2^{(k)}r)+K_2(q_2^{(k)}r))+\right.$$
$$\left.\frac{\lambda^{(k)}}{2\mu^{(k)}}(-\frac{sq_2^{(k)}}{r}K_1(q_2^{(k)}r)-sq_2^{(k)}K_0(q_2^{(k)}r))\right]\Bigg],$$
$$\sigma_{\theta\theta F}^{(k)}=2\mu^{(k)}\left[A_1^{(k)}\left[\frac{\lambda^{(k)}}{2\mu^{(k)}}\ ((q_1^{(k)})^2 0.5(I_0(q_1^{(k)}r)+I_2(q_1^{(k)}r))-\right.\right.$$
$$\left.s^2 I_0(q_1^{(k)}r))+(1+\frac{\lambda^{(k)}}{2\mu^{(k)}})\frac{q_1^{(k)}}{r}I_1(q_1^{(k)}r)\right]+$$
$$A_2^{(k)}\left[\frac{\lambda^{(k)}}{2\mu^{(k)}}\ ((q_1^{(k)})^2 0.5(K_0(q_1^{(k)}r)+K_2(q_1^{(k)}r))-s^2K_0(q_1^{(k)}r))+\right.$$
$$\left.(1+\frac{\lambda^{(k)}}{2\mu^{(k)}})(-\frac{q_1^{(k)}}{r}K_1(q_1^{(k)}r))\right]+$$
$$B_1^{(k)}\left[\frac{\lambda^{(k)}}{2\mu^{(k)}}\ (s(q_2^{(k)})^2 0.5(I_0(q_2^{(k)}r)+I_2(q_2^{(k)}r))-sq_2^{(k)}I_0(q_2^{(k)}r))+\right.$$
$$\left.(1+\frac{\lambda^{(k)}}{\mu^{(k)}})\frac{sq_2^{(k)}}{r}I_1(q_2^{(k)}r)\right]+$$
$$B_2^{(k)}\left[\frac{\lambda^{(k)}}{2\mu^{(k)}}\ (s(q_2^{(k)})^2 0.5(K_0(q_2^{(k)}r)+K_2(q_2^{(k)}r))-sq_2^{(k)}K_0(q_2^{(k)}r))+\right.$$
$$\left.(1+\frac{\lambda^{(k)}}{\mu^{(k)}})(-\frac{sq_2^{(k)}}{r}K_1(q_2^{(k)}r))\right]\Bigg],$$
$$\sigma_{zzF}^{(k)}=2\mu^{(k)}\left[A_1^{(k)}\left[\frac{\lambda^{(k)}}{2\mu^{(k)}}\ ((q_1^{(k)})^2 0.5(I_0(q_1^{(k)}r)+I_2(q_1^{(k)}r))+\right.\right.$$
$$\left.\frac{q_1^{(k)}}{r}I_1(q_1^{(k)}r))-(1+\frac{\lambda^{(k)}}{2\mu^{(k)}})s^2I_0(q_1^{(k)}r))\right]+$$
$$A_2^{(k)}\left[\frac{\lambda^{(k)}}{2\mu^{(k)}}\ ((q_1^{(k)})^2 0.5(K_0(q_1^{(k)}r)+K_2(q_1^{(k)}r))-\frac{q_1^{(k)}}{r}K_1(q_1^{(k)}r))-\right.$$
$$\left.(1+\frac{\lambda^{(k)}}{2\mu^{(k)}})s^2K_0(q_1^{(k)}r)\right]+$$
$$B_1^{(k)}\left[\frac{\lambda^{(k)}}{2\mu^{(k)}}\ (s(q_2^{(k)})^2 0.5(I_0(q_2^{(k)}r)+I_2(q_2^{(k)}r))+\right.$$
$$\left.\frac{sq_2^{(k)}}{r}I_1(q_2^{(k)}r))-(1+\frac{\lambda^{(k)}}{2\mu^{(k)}})sq_2^{(k)}I_0(q_2^{(k)}r)\right]+$$
$$B_2^{(k)}\left[\frac{\lambda^{(k)}}{2\mu^{(k)}}\ (s(q_2^{(k)})^2 0.5(K_0(q_2^{(k)}r)+K_2(q_2^{(k)}r))-\frac{sq_2^{(k)}}{r}K_1(q_2^{(k)}r))-\right.$$

$$(1+\frac{\lambda^{(k)}}{2\mu^{(k)}})sq_2^{(k)}K_0(q_2^{(k)}r)\Big]\Big], k=1,2. \tag{18}$$

Thus, using the expressions in (18) we attempt to satisfy the Fourier transformations of the conditions (13) and (4) – (6), according to which, the following expressions can be written.

$$\sigma_{rrF}^{(2)}\Big|_{r=R-h_2} = -P_0 \Rightarrow \alpha_{11}A_1^{(2)}+\alpha_{12}A_2^{(2)}+\alpha_{13}B_1^{(2)}+\alpha_{14}B_2^{(2)}+$$

$$\alpha_{15}A_1^{(1)}+\alpha_{16}A_2^{(1)}+\alpha_{17}B_1^{(1)}+\alpha_{18}B_2^{(1)} = -P_0,$$

$$\sigma_{rzF}^{(2)}\Big|_{r=R-h_2} = 0 \Rightarrow \alpha_{21}A_1^{(2)}+\alpha_{22}A_2^{(2)}+\alpha_{23}B_1^{(2)}+\alpha_{24}B_2^{(2)}+$$

$$\alpha_{25}A_1^{(1)}+\alpha_{26}A_2^{(1)}+\alpha_{27}B_1^{(1)}+\alpha_{28}B_2^{(1)} = 0,$$

$$\sigma_{rr}^{(1)}\Big|_{r=R} = \sigma_{rr}^{(2)}\Big|_{r=R} \Rightarrow \alpha_{31}A_1^{(2)}+\alpha_{32}A_2^{(2)}+\alpha_{33}B_1^{(2)}+\alpha_{34}B_2^{(2)}+$$

$$\alpha_{35}A_1^{(1)}+\alpha_{36}A_2^{(1)}+\alpha_{37}B_1^{(1)}+\alpha_{38}B_2^{(1)} = 0,$$

$$\sigma_{rz}^{(1)}\Big|_{r=R} = \sigma_{rz}^{(2)}\Big|_{r=R} \Rightarrow \alpha_{41}A_1^{(2)}+\alpha_{42}A_2^{(2)}+\alpha_{43}B_1^{(2)}+\alpha_{44}B_2^{(2)}+$$

$$\alpha_{45}A_1^{(1)}+\alpha_{46}A_2^{(1)}+\alpha_{47}B_1^{(1)}+\alpha_{48}B_2^{(1)} = 0,$$

$$u_r^{(1)}\Big|_{r=R} = u_r^{(2)}\Big|_{r=R} \Rightarrow \alpha_{51}A_1^{(2)}+\alpha_{52}A_2^{(2)}+\alpha_{53}B_1^{(2)}+\alpha_{54}B_2^{(2)}+$$

$$\alpha_{55}A_1^{(1)}+\alpha_{56}A_2^{(1)}+\alpha_{57}B_1^{(1)}+\alpha_{58}B_2^{(1)} = 0,$$

$$u_z^{(1)}\Big|_{r=R} - u_z^{(2)}\Big|_{r=R} = \frac{FR}{\mu^{(1)}}\sigma_{rz}^{(1)}\Big|_{r=R} \Rightarrow \alpha_{61}A_1^{(2)}+\alpha_{62}A_2^{(2)}+\alpha_{63}B_1^{(2)}+\alpha_{64}B_2^{(2)}+$$

$$\alpha_{65}A_1^{(1)}+\alpha_{66}A_2^{(1)}++\alpha_{67}B_1^{(1)}+\alpha_{68}B_2^{(1)} = 0,$$

$$\sigma_{rrF}^{(1)}\Big|_{r=R+h_1} = 0 \Rightarrow \alpha_{75}A_1^{(1)}+\alpha_{76}A_2^{(1)}+\alpha_{77}B_1^{(1)}+\alpha_{78}B_2^{(1)} = 0,$$

$$\sigma_{rzF}^{(1)}\Big|_{r=R+h_1} = 0 \Rightarrow \alpha_{85}A_1^{(1)}+\alpha_{86}A_2^{(1)}+\alpha_{87}B_1^{(1)}+\alpha_{88}B_2^{(1)} = 0. \tag{19}$$

The coefficients α_{ij}, where $i;j = 1,2,3,...,8$ can be easily determined from the expressions in (18).

Thus, solving the equations in (19) with respect to the unknowns $A_1^{(2)}, A_2^{(2)}, B_1^{(2)}$, $B_2^{(2)}$, $A_1^{(1)}, A_2^{(1)}, B_1^{(1)}$, and $B_2^{(1)}$ we determine completely the Fourier transformations of all the sought values and, substituting these values into the integrals in (14) and calculating these integrals, we determine the originals of the stresses and displacements in the system under consideration caused by the action of the external moving load.

This completes the consideration of the solution method.

4. Numerical results and discussions

4.1. **The criteria and algorithm for calculation of the critical velocity.** First, we consider the criterion for determination of the critical velocity under which the values of the stresses and displacements become infinity and resonance-type behavior occurs. For this purpose, we detail the expressions of the unknown constants $A_1^{(2)}, A_2^{(2)}, B_1^{(2)}, B_2^{(2)}, A_2^{(1)}, A_1^{(1)}, A_2^{(1)}, B_1^{(1)}$, and $B_2^{(1)}$ which are obtained from the equation (19) and can be presented as follows:

$$\left\{A_1^{(2)}; A_2^{(2)}; B_1^{(2)}; B_2^{(2)}; A_2^{(1)}; A_2^{(2)}; B_1^{(2)}; B_2^{(1)}\right\} = \frac{1}{\det\|\alpha_{ij}\|}\left\{\det\left\|\beta_{ij}^{A_1^{(2)}}\right\|; \det\left\|\beta_{ij}^{A_2^{(2)}}\right\|;\right.$$

$$\left.\det\left\|\beta_{ij}^{B_1^{(2)}}\right\|; \det\left\|\beta_{ij}^{B_2^{(2)}}\right\|; \det\left\|\beta_{ij}^{A_1^{(1)}}\right\|; \det\left\|\beta_{ij}^{A_2^{(1)}}\right\|; \det\left\|\beta_{ij}^{B_1^{(1)}}\right\|; \det\left\|\beta_{ij}^{B_2^{(1)}}\right\|\right\}, \tag{20}$$

where the matrices $\left(\beta_{ij}^{A_1^{(2)}}\right)$, $\left(\beta_{ij}^{A_2^{(2)}}\right)$, $\left(\beta_{ij}^{B_1^{(2)}}\right)$, $\left(\beta_{ij}^{B_2^{(2)}}\right)$, $\left(\beta_{ij}^{A_1^{(1)}}\right)$ $\left(\beta_{ij}^{A_2^{(1)}}\right)$, $\left(\beta_{ij}^{B_1^{(1)}}\right)$ and $\left(\beta_{ij}^{B_2^{(1)}}\right)$ are obtained from the matrix (α_{ij}) by replacing the first, second, third, fourth, fifth, sixth, seventh and eighth columns with the column $(-P_0\ , 0, 0, 0, 0\ , 0)^T$, respectively.

At the same time, for the selected value of the load moving velocity V, the equation

$$\det\|\alpha_{ij}\| = 0 \tag{21}$$

has roots with respect to the Fourier transformation parameter s and as a result of the solution of the equation (21), the relation $V = V(s)$ is obtained. It is obvious that if the order of this root is one, then the integrals in (14) at the vicinity of this root can be calculated in Cauchy's principal value sense. However, if there is a root the order of which is two, then the integrals in (14) have infinite values and namely the velocities corresponding to this root are called the critical velocity. In other words, the critical velocity is determined as the velocity corresponding to the case where

$$\frac{dV}{ds} = 0. \tag{22}$$

It should also be noted that if we rename the Fourier transformation parameter s with the wavenumber and the load moving velocity with the wave propagation velocity, then the equation (21) coincides with the dispersion equation of the corresponding axisymmetric wave propagation problem. So, the relation $V = V(s)$ obtained from the solution of the equation (21), which is made by employing the well-known "bisection" method, is also the dispersion relation of the axisymmetric longitudinal waves in the bi-layered hollow cylinder under consideration. Therefore, in some investigations (for instance in the paper by Abdulkadirov [1]) the critical velocity is renamed as "resonance waves" and is determined from the dispersion curves of the corresponding wave propagation problem.

This completes the consideration of the criteria and algorithm for determination of the critical velocity under which the resonance-type phenomenon takes place.

4.2. **Algorithm for calculation of the integrals in (14).** First of all we note that the integrals in (14) and similar types of integrals are called wavenumber integrals, for calculation of which, special algorithms are employed. These algorithms are discussed in the works [5, 26, 32] and others listed therein. According to these discussions, in the present investigation we prefer to apply the Sommerfeld contour integration method. This method is based on Cauchy's theorem on the values of the analytic functions over the closed contour, and according to this

theorem the contour $[0,+\infty]$ is "deformed" into the contour C (Fig. 2), which is called the Sommerfeld contour in the complex plane $s = s_1 + is_2$ and in this way the real roots of the equation (21) are avoided under calculation of the wavenumber integrals.

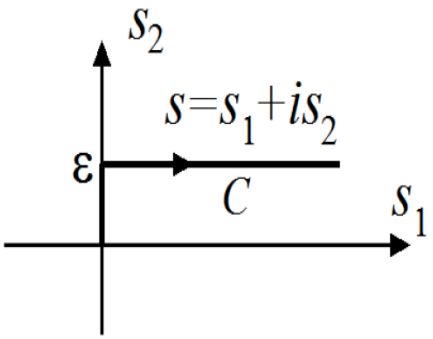

Figure 2. The sketch of the Sommerfeld contour.

Thus, according to this method, the integrals in (14) are transformed into the following ones.

$$\left\{\Phi^{(k)}; u_r^{(k)}; \sigma_{nn}^{(k)}; \varepsilon_{nn}^{(k)}\right\}(r,z) = \frac{1}{\pi} Re \int_C \left\{\Phi_F^{(k)}; u_{rF}^{(k)}; \sigma_{nnF}^{(k)}; \varepsilon_{nnF}^{(k)}\right\}(r,s)\cos(sz)ds, nn = rr;\ \theta\theta;\ zz$$

$$\left\{\Psi^{(k)}; u_z^{(k)}; \sigma_{rz}^{(k)}; \varepsilon_{rz}^{(k)};\right\}(r,z) = \frac{1}{\pi} Re \int_C \left\{\Psi_F^{(k)}; u_{zF}^{(k)}; \sigma_{rzF}^{(k)}; \varepsilon_{rzF}^{(k)}\right\}(r,s)\sin(sz)ds. \tag{23}$$

Taking the configuration of the contour C given in Fig. 2, we can write the following relations.

$$\int_C f(s)\cos(sz)ds = \int_0^\infty f(s_1+i\varepsilon_2)\cos(s_1+i\varepsilon_2)ds_1 + i\int_0^\varepsilon f(is_2)\cos(is_2)ds_2,$$

$$\int_C f(s)\sin(sz)ds = \int_0^\infty f(s_1+i\varepsilon_2)\sin(s_1+i\varepsilon_2)ds_1 + i\int_0^\varepsilon f(is_2)\sin(is_2)ds_2. \tag{24}$$

Assuming that $\varepsilon \ll 1$, we can neglect the integrals with respect to s_2 in (24) and obtain the following expressions for calculation of the integrals in (23).

$$\left\{\Phi^{(k)}; u_r^{(k)}; \sigma_{nn}^{(k)}; \varepsilon_{nn}^{(k)}\right\}(r,z) \approx \frac{1}{\pi} Re \int_0^{+\infty} \left\{\Phi_F^{(k)}; u_{rF}^{(k)}; \sigma_{nnF}^{(k)}; \varepsilon_{nnF}^{(k)}\right\}(r, s_1+i\varepsilon)\cos((s_1+i\varepsilon)z)ds_1,$$

$$[\left\{\Psi^{(k)}; u_z^{(k)}; \sigma_{rz}^{(k)}; \varepsilon_{rz}^{(k)};\right\}(r,z) \approx \frac{1}{\pi} Re \int_0^{+\infty} \left\{\Psi_F^{(k)}; u_{zF}^{(k)}; \sigma_{rzF}^{(k)}; \varepsilon_{rzF}^{(k)}\right\}(r, s_1+is_2)\sin((s_1+i\varepsilon)z)ds_1. \tag{25}$$

Under calculation of the integrals in (25) the improper integral $\int_0^{+\infty}(\bullet)ds_1$ is replaced with the corresponding definite integral $\int_0^{S_1^*}(\bullet)ds_1$ and the values of S_1^* are determined from the corresponding convergence requirement. Moreover, under calculation of the integral $\int_0^{S_1^*}(\bullet)ds_1$, the

interval $[0, S_1^*]$ is divided into a certain number (denote this number through N) of shorter intervals and within each of these shorter intervals the integrals are calculated by the use of the Gauss algorithm with ten integration points. The values of the integrated functions at these integration points are calculated through the solution of the equation (19) and it is assumed that in each of the shorter intervals the sampling interval Δs_1 of the numerical integration must satisfy the relation $\Delta s_1 \ll \min\{\varepsilon, 1/z\}$. All these procedures are performed automatically in the PC by the use of the corresponding programs constructed by the authors of the present paper in MATLAB.

4.3. **Numerical results related to the critical velocity.** All numerical results which will be considered in the present subsection are obtained through the solution to the equation (21). First, we consider the numerical results obtained in the following four cases:

$$Case\ \ 1: \frac{E^{(1)}}{E^{(2)}} = 0.35, \nu^{(1)} = \nu^{(2)} = 0.25, \frac{\rho^{(1)}}{\rho^{(2)}} = 0.1; \tag{26}$$

$$Case\ \ 2: \frac{E^{(1)}}{E^{(2)}} = 0.05, \nu^{(1)} = \nu^{(2)} = 0.25, \frac{\rho^{(1)}}{\rho^{(2)}} = 0.01. \tag{27}$$

$$Case\ \ 3: \frac{E^{(1)}}{E^{(2)}} = 0.02, \nu^{(1)} = \nu^{(2)} = 0.25, \frac{\rho^{(1)}}{\rho^{(2)}} = 0.01. \tag{28}$$

$$Case\ \ 4: \frac{E^{(1)}}{E^{(2)}} = 0.01, \nu^{(1)} = \nu^{(2)} = 0.25, \frac{\rho^{(1)}}{\rho^{(2)}} = 0.01. \tag{29}$$

Note that Case 1 and Case 2 were also considered in the paper by Abdulkadirov [1] within the assumption that $h_2/R = 0.5$ and $h_1/R = \infty$(i.e. in the paper [1] the system consisting of the hollow cylinder and surrounding infinite elastic medium is considered) and the existence of the critical velocity was observed in Case 1 (in Case 2) under $F = \infty$ (under $F = 0$) in (6), i.e. under full slipping imperfect (perfect) contact conditions between the hollow cylinder and surrounding elastic medium. In the present investigation we obtain numerical results not only for the cases where $F = 0$ and $F = \infty$, but also for the cases where $0 < F < +\infty$ in which obtained numerical results are more meaningful.

Thus, we consider numerical results related to the dimensionless critical velocity $c_{cr} = V_{cr}/c_2^{(2)}$ (where $c_2^{(2)} = \sqrt{\mu^{(2)}/\rho^{(2)}}$) and obtained in the foregoing cases indicated through the relations Case 1-4. These results are given in Tables 1, 2. 3 and 4 which relate to Case 1, Case 2, Case 3 and Case 4 respectively and are obtained in the cases where $F = 0$ (upper number) and $F = \infty$ (lower number). Note that in Tables 1 and 2 it is also indicated the corresponding results obtained in the work [1]. Moreover, note that the results given in the aforementioned tables are obtained for various values of the ratios h_1/R and h_2/R.

Table 1. The values of the dimensionless critical velocity c_{cr} $(= V_{cr}/c_2^{(2)})$ in Case 1 under the perfect contact (upper number) and imperfect-full slipping contact (lower number) between the cylinders.

h_2/R	h_1/R						
	0.1	0.3	0.5	1.0	2.5	5.5	∞
0.5	0.8375 0.7903	0.9160 0.8133	0.9350 0.8559	0.9355 0.8807	0.9355 0.8809	0.9355 0.8809	0.9355 0.8809 [1]
0.3	0.7064 0.6396	0.8369 0.6930	0.8864 0.7729	0.8881 0.8027	0.8881 0.8028	0.8881 0.8028	0.8881 0.8028
0.1	0.5439 0.4177	0.8159 0.6592	0.8437 0.7310	0.8437 0.7311	0.8437 0.7311	0.8437 0.7311	0.8437 0.7311

Table 2. The values of the dimensionless critical velocity c_{cr} $(= V_{cr}/c_2^{(2)})$ in Case 2 under the perfect contact (upper number) and imperfect-full slipping contact (lower number) between the cylinders.

h_2/R	h_1/R						
	0.1	0.3	0.5	1.0	2.5	5.5	∞
0.5	0.8003 0.7917	0.8173 0.7961	0.8238 0.8037	0.8260 0.8099	0.8261 0.8101	0.8261 0.8101	0.8261 [1] 0.8101
0.3	0.6501 0.6374	0.6801 0.6472	0.6930 0.6624	0.6977 0.6735	0.6977 0.6738	0.6977 0.6738	0.6977 0.6738
0.1	0.4223 0.3869	0.5112 0.4502	0.5279 0.4867	0.5291 0.4900	0.5291 0.4900	0.5291 0.4900	0.5291 0.4900

Table 3. The values of the dimensionless critical velocity c_{cr} $(= V_{cr}/c_2^{(2)})$ in Case 3 under the perfect contact (upper number) and imperfect-full slipping contact (lower number) between the cylinders.

h_2/R	h_1/R						
	0.1	0.3	0.5	1.0	2.5	5.5	∞
0.5	0.7945 0.7911	0.8010 0.7917	0.8038 0.7944	0.8052 0.7978	0.8052 0.7981	0.8052 0.7981	0.8052 0.7981
0.3	0.6413 0.6362	0.6532 0.6388	0.6588 0.6446	0.6615 0.6505	0.6615 0.6508	0.6615 0.6508	0.6615 0.6508
0.1	0.3970 0.3815	0.4365 0.4069	0.4474 0.4259	0.4490 0.4296	0.4490 0.4296	0.4490 0.4296	0.4490 0.4296

Table 4. The values of the dimensionless critical velocity c_{cr} $(= V_{cr}/c_2^{(2)})$ in Case 4 under the perfect contact (upper number) and imperfect-full slipping contact (lower number) between the cylinders.

h_2/R	h_1/R						
	0.1	0.3	0.5	1.0	2.5	5.5	∞
0.5	0.7925 0.7809	0.7952 0.7901	0.7966 0.7904	0.7976 0.7929	0.7977 0.7936	0.7977 0.7936	0.7977 0.7936
0.3	0.6383 0.6358	0.6436 0.6358	0.6464 0.6381	0.6482 0.6420	0.6482 0.6424	0.6483 0.6424	0.6483 0.6424
0.1	0.3877 0.3797	0.4078 0.3912	0.4144 0.4019	0.4157 0.4048	0.4157 0.4049	0.4157 0.4049	0.4157 0.4049

It follows from the analysis of the numerical results that an increase in the values of the h_1/R and h_2/R cases an increase in the values of the critical velocity. Moreover, according to the mechanical consideration, as we consider the subsonic regime of the moving load (8), the values of the critical velocity must approach a certain limit with h_1/R and this limit is the critical velocity correspondence to that related to the system consisting of the hollow cylinder and surrounding elastic medium. Data given in Tables 1 – 4 and obtained for various h_1/R proves this consideration and the mentioned limit values coincide with the known ones obtained in the paper [1]. Consequently, this coinciding proves also the validity and trustiness of the calculation algorithm and PC programs used in the present investigation and realized in MATLAB.

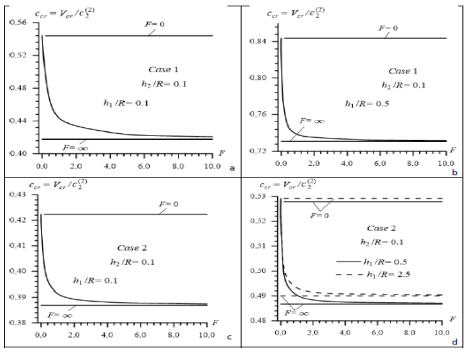

Figure 3. The dependence of the critical velocity on the imperfection parameter F in Case 1 (26) under $h_1/R = 0.1(a)$, $h_2/R = 0.1(b)$, and in Case 2 (27) under $h_1/R = 0.5(c)$, and $h_2/R = 0.5(d)$.

Analysis of the data given in Tables 2, 3 and 4 allows us to conclude that an increase in the modulus of elasticity of the inner layer material under fixed modulus of elasticity of the external layer material causes a decrease in the values of the dimensionless critical velocity c_{cr} $(= V_{cr}/c_2^{(2)})$. Moreover, this analysis allows us to conclude that the full-slipping type imperfectness of the contact conditions between the layers of the cylinder causes decrease significantly of the values of the critical velocity.

Numerical investigations show that the critical velocities obtained in the cases where $0<F<\infty$ are limited with corresponding ones obtained in the cases where $F = 0$ (upper limit) and $F = \infty$ (lower limit). For illustration this statement we consider the graphs of the dependence between c_{cr} and the parameter F constructed in the case where $h_2/R = 0.1$ and given in Fig.3 for Case 1(Figs. 3a and 3b) and Case 2 (Figs. 3c and 3d) for $h_1/R = 0.1$ (Figs. 3a and 3c), 0.5 (Figs. 3b and 3d) and 2.5 (Fig. 3d).

It follows from the results given in Fig. 3 that the values of the critical velocity decrease monotonically with the parameter F and in the quantitative sense the main decrease in the values of the c_{cr} appears under $0 < F < 2.0$. Note that similar type results are also obtained for the other values of the problem parameters and for Case 3 and Case 4.

This completes the consideration of the numerical results related to the critical velocity.

4.4. **Numerical results related to the stress distributions.** The results discussed in the present subsection are obtained within the scope of the algorithm described in the subsection 4.2. First of all, we note on the convergence of the values of the integrals in (25) with respect to N and S_1^* in the cases where $V < V_{cr}$.

According to the conditions in (8), in the cases where $V < V_{cr}$ the integrated expressions do not have any singularity over an arbitrary integrated interval $[0, S_1^*]$. However, in this case the integrated expressions have the fast oscillating terms - $\cos(sz)$ or $\sin(sz)$, and this also causes difficulties in the convergence sense of the integrals in (25). This difficulty can also be prevented by the use of the Sommerfeld contour integration method which is also used in the present study.

As a result of the corresponding numerical investigations, it is established that in the accuracy and convergence senses it is enough to assume that $10^{-300} \leq \varepsilon \leq 0.01$ in the integrals in (25). Note that the values of the integrals calculated for each value of the parameter ε selected from the interval $\left[10^{-300}, 0.01\right]$ coincide with each other with accuracy $10^{-7} - 10^{-9}$. Under obtaining the numerical results considered below, it is assumed that $\varepsilon = 0.0001$.

It should also be noted that under using the Sommerfeld contour integration method in the cases where $V < V_{cr}$ there is no difficulty in convergence of the integrals in (25) with respect to the values of N and the results obtained for the case where $N = 1$ coincide with the results obtained for each case where $N > 1$. We recall that N shows the number of the shorter integration intervals, the summation of which gives the interval $[0, S_1^*]$. Thus, in the cases under consideration, there is no meaning to the convergence of the numerical results with respect to the number N. Therefore, the convergence of the numerical results with respect to the length of the integration interval, i.e. with respect to the values of S_1^* can be verified. As such verifications are considered in many related investigations and discussed in the monograph [5], therefore we here do not consider numerical examples illustrating the convergence of the numerical results with respect to the S_1^*. Nevertheless, we note that under obtaining numerical results which will be discussed below it is assumed that $S_1^* = 9$.

Thus, we consider numerical results related to the response of the interface normal $\sigma_{rr}(z) = \sigma_{rr}^{(1)}(R, z) = \sigma_{rr}^{(2)}(R, z)$ and shear $\sigma_{rz}(z) = \sigma_{rz}^{(1)}(R, z) = \sigma_{rz}^{(2)}(R, z)$ stresses to the dimensionless velocity $c = V/c_2^{(2)}$ of the moving load and for this purpose we examine the Case 1

and Case 2 only. Consider graphs given in Figs. 4 (Case 1) and 5 (Case 2) which illustrate the response of the dimensionless normal stress $\sigma_{rr}h_2/P_0$ calculated at $z/h_2 = 0$ to the load moving velocity c in the cases where $h_2/R = 0.1$(a), 0.3 (b) and 0.5 (c) for various values of the ratio h_1/R. Also consider graphs given in Figs. 6 (Case 1) which illustrate the response of the dimensionless shear stress $\sigma_{rz}h_2/P_0$ calculated at $z/h_2 = 0.5$ to the load moving velocity c in the cases where $h_2/R = 0.1$(a), 0.3 (b) and 0.5 (c) for various values of the ratio h_1/R. Note that all the results given in Figs. 5 and 6 are obtained in the perfect contact case, i.e. in the case where $F = 0$.

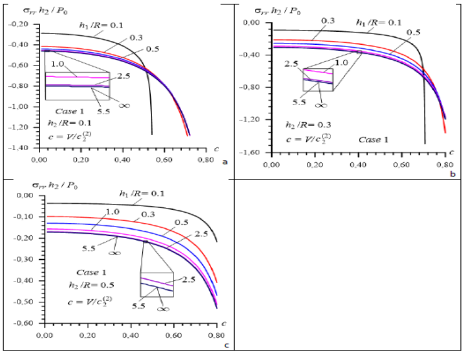

Figure 4. Response interface normal stress to the load moving velocity in Case 1 calculated for various h_1/R under $h_2/R = 0.5(a), 0.1\ 0.3(b)$ and 0.5.

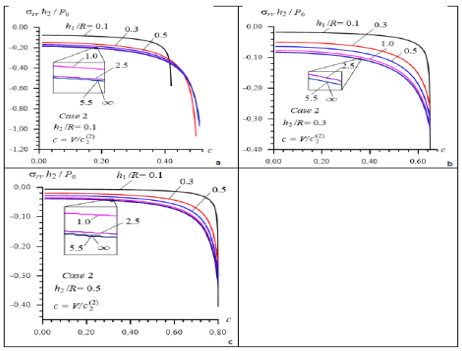

Figure 5. Response interface normal stress to the load moving velocity in Case 2 calculated for various h_1/R under $h_2/R = 0.1(a)$, $0.3(b)$ and 0.5.

Figs. 5 and 6 show that the absolute values of the interface stresses increase monotonically with the load moving velocity. At the same time, these figures show that in the cases where the load moving velocity is "far from" the corresponding critical velocity the absolute values of the interface normal stress decrease with decreasing of the thickness of the external layer of the cylinder. However, in the cases where the load moving velocity is a "near" with the corresponding critical velocity the absolute values of this stress increase with decreasing of the mentioned thickness. Moreover, in the latter case not only absolute values of the interface normal stress, but also absolute values of the interface shear stress increase with decreasing of the external layer thickness. This is because a decrease in the thickness of the external layer causes a decrease in the values of the critical velocity.

Note that as will be shown below, absolute maximum values of the interface normal stress with respect to the coordinate z/h_2 appear at $z/h_2 = 0$. However the coordinate z/h_2 at which the absolute value of the interface shear stress has its maximum depends on the h_1/R. As in all

the cases shown in Fig. 6 the values of the shear stress are calculated at $z/h_2 = 0.5$, therefore it is difficult to make any correct conclusion on the influence of the h_1/R on the absolute values of the shear stress from the results given in Fig. 6.

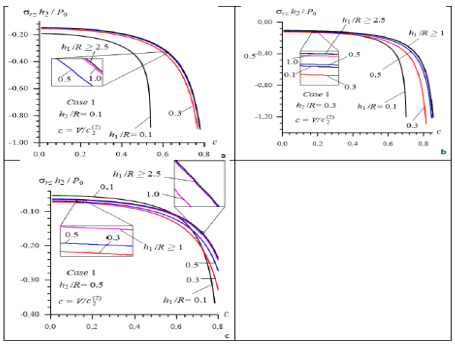

Figure 6. Response interface shear stress to the load moving velocity in Case 1 calculated for various h_1/R under $h_2/R = 0.1(a)$, $0.3(b)$ and 0.5.

We recall that the results given in Figs. 5 and 6 are obtained in the case where $F = 0$. Now we consider the results illustrated how the parameter F acts on the response of the interface stress to the load moving velocity. We examine this influence with respect to the interface normal stress in Case 1 under $h_2/R = 0.1$ for various values of the ratio h_1/R. Note that related results are given in Fig. 7 from which follows that in the cases where the load moving velocity is "far from" the corresponding critical velocity the absolute values of the normal stress decrease with the parameter F. However in the cases where the load moving velocity is a near to the corresponding critical velocity, an increase in the values of the parameter F causes an increase in the absolute values of this stress. It is evident that this character of the influence of the parameter F on the studied responses can be explained with decreasing of the critical velocity under increasing of the parameter F.

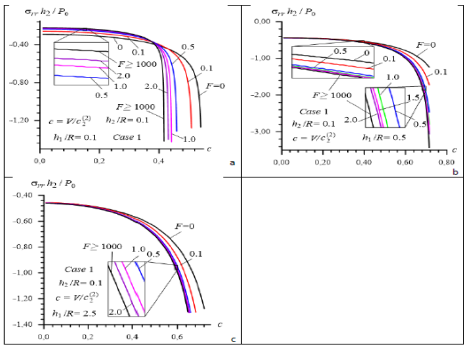

Figure 7. The influence of the imperfection parameter on the response of the interface normal stress to the load moving velocity in Case 1 under $h_1/R = 0.1(a)$, $0.5(b)$ and $2.5(c)$ for $h_2/R = 0.1$.

Now we consider numerical results related to the distribution of the interface stresses with respect to the coordinate z/h_2 and examine this distribution with the results related to Case 2 and obtained in the cases where $h_2/R = 0.3$and 05 for various values of the ratio h_1/R under $F = 0$.Graphs of this distribution of the interface normal (shear) stress are given in Fig. 8 (in Fig. 9) and the graphs in this figure grouped with the letter a (with the letter b) show the results obtained in the case where $h_2/R = 0.3$ (in the case where $h_2/R = 0.5$). Thus, it follows

from these graphs that the absolute values of the studied stresses decrease with distance from the point at which the moving load acts. Moreover, these graphs show that the magnitude of the decaying of the stresses with the distance from the moving load acting point increases with the thickness of the external and inner layers of the cylinder.

We recall that the z in the Figs. 8 and 9 is the coordinate in the moving coordinate system determined through the relations in (11). Thus, according to the relations in (11), the graphs given in Figs. 8 and 9 can be considered as a change of the studied quantities with time at a fixed point in the fixed coordinate system.

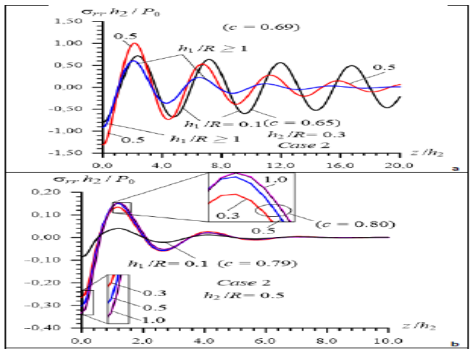

Figure 8. Distribution of the interface normal stress with respect to the distance from the moving load in Case 2 for various h_1/R under $h_2/R = 0.3(a)$, and $0.5(b)$.

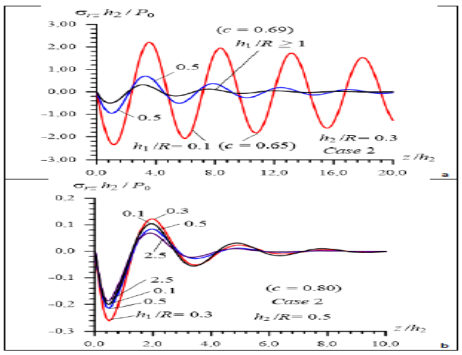

Figure 9. Distribution of the interface shear stress with respect to the distance from the moving load in Case 2 for various h_1/R under $h_2/R = 0.3(a)$, and $0.5(b)$.

5. Conclusions

Thus, in the present paper the dynamics of the moving axisymmetric ring load which is point located with respect to the cylinder axis and acts on the internal face of the bi-layered hollow cylinder has been investigated within the scope of the piecewise homogeneous body model by employing the exact equations of elastodynamics. It is assumed that the contact conditions between the layers of the cylinder have shear-spring type imperfection. The subsonic regime is considered and for solution of the corresponding boundary value problem both the method of the moving coordinate system and the Fourier transformation, with respect to the coordinate directed along the cylinder axis in the moving coordinate system, are applied. Analytical expressions for the Fourier transformations of the sought values are determined and the algorithm for determination of the critical velocity and inverse Fourier transformations are discussed. Numerical results on the critical velocity and the stress distribution on the interface surface between

the cylinder and surrounding elastic medium are presented and discussed. Analyses of these numerical results allow us to make the following concrete conclusions:

(1) The values of the critical velocity depends significantly on the whole thickness of the bi-layered hollow cylinder and increase with this thickness;
(2) An increase in the thickness of the external layer of the cylinder causes an increase in the values of the critical velocity and approach this velocity the corresponding one obtained for the system consisting of the hollow cylinder and surrounding infinite elastic medium;
(3) The values of the dimensionless critical velocity c_{cr} $(= V_{cr}/c_2^{(2)})$ decrease with increasing of the modulus of elasticity of the inner layer material of the cylinder;
(4) The values of the critical velocity decrease monotonically with increasing of the parameter F which characterized the degree of the imperfectness of the contact conditions and approach the corresponding one obtained in the full-slipping imperfect contact case;
(5) The values of the critical velocity decrease with increasing of the external radius of the cross section of the inner layer-cylinder under constant whole thickness of the cylinder;
(6) The absolute values of the interface normal and shear stresses increase monotonically with load moving velocity;
(7) In the cases where the load moving velocity is far from the corresponding critical velocity the absolute values of the interface normal stresses increase with the external layer thickness, however in the cases where the load moving velocity is a near to the critical velocity the absolute values of the interface stresses increase with a decreasing of the external layer thickness;
(8) The attenuation of the interface stresses with respect to time (or with the distance from the point at which the moving load acts) becomes more significant with increasing of the layers thickness of the cylinder.

References

[1] Abdulkadirov, S.A., (1981), Low-frequency resonance waves in a cylindrical layer surrounded by an elastic medium, Journal of Mining Sci., 80, pp.229-234.
[2] Achenbach, J.D., Keshava, S.P., Hermann, G., (1967), Moving load on a plate resting on an elastic half space, Trans ASME Ser E J. Appl. Mech., 34(4), pp.183-189.
[3] Akbarov, S.D., (2010), Dynamical (time-harmonic) axisymmetric stress field in the pre-stretched non-linear elastic bi-layered slab resting on the rigid foundation, TWMS J. Pure Appl. Math., 1(2), pp.146-154.
[4] Akbarov, S.D., (2013), On the axisymmetric time-harmonic Lamb's problem for a system comprising a half-space and a covering layer with finite initial strains, CMES: Comp. Model. Eng. Sci., 95(3), pp.143-175.
[5] Akbarov, S.D., (2015), Dynamics of Pre-Strained Bi-Material Elastic Systems: Linearized Three-Dimensional Approach, Springer, New-York, 1004p.
[6] Akbarov, S.D., Guler, C., Dincoy, E., (2007), The critical speed of a moving load on a pre-stressed load plate resting on a pre-stressed half-plan, Mech. Comp. Mater., 43(2), pp.173-182.
[7] Akbarov, S.D., Salmanova, K.A., (2009), On the dynamics of a finite pre-strained bi-layered slab resting on a rigid foundation under the action of an oscillating moving load, J. Sound. Vibr., 327(3-5), pp.454-472.
[8] Akbarov, S.D., Ilhan, N., (2008), Dynamics of a system comprising a pre-stressed orthotropic layer and pre-stressed orthotropic half-plane under the action of a moving load, Int. J. Solid. Str., 45(14-15), pp.4222-4235.
[9] Akbarov, S.D., Ilhan, N., (2009), Dynamics of a system comprising an orthotropic layer and orthotropic half-plane under the action of an oscillating moving load, Int. J. Solid. Str., 46(21), pp.3873-3881.
[10] Akbarov, S.D., Ilhan, N., Temugan, A., (2015), 3D Dynamics of a system comprising a pre-stressed covering layer and a pre-stressed half-space under the action of an oscillating moving point-located load, Appl. Math. Model., 39(1), pp.1-18.

[11] Akbarov, S.D., Ismailov M.I., (2015), Dynamics of the moving load acting on the hydro-elastic system consisting of the elastic plate, compressible viscous fluid and rigid wall, CMC- Comput. Mater. Contin., 45(2), pp.75-105.
[12] Akbarov, S.D., Ismailov M.I., (2016), Frequency response of a pre-stressed metal elastic plate under compressible viscous fluid loading, Appl. Comput. Math., 15(2), pp.172-188.
[13] Aliyev, F.A., Larin, V.B., Veliyeva, N.I., Gasimova, K., Faradjova, Sh.A., (2019), Algorithm for solving the systems of the generalized Sylvester transpose matrix equations using LMI, TWMS J. Pure Appl. Math., 10(2), pp.239-245.
[14] Aman, T., Ishak, A., (2014), Stagnation-point flow and heat transfer over a nonlinearly stretching sheet in a micropolar fluid with viscous dissipation, Appl. Comput. Math., 13(2), pp.230-238.
[15] Ashraf, M., Asghar, S., Hossain, M.A., (2014), The computational study of the effects of magnetic field and free stream velocty oscillation on boundary layer flow past a magnetized vertical plate, Appl. Comput. Math., 13(2), pp.175-193.
[16] Babich, S.Y., Glukhov, Y.P., Guz, A.N., (1986), Dynamics of a layered compressible pre-stressed half-space under the influence of moving load, Int. Appl. Mech., 22(6), pp.808-815.
[17] Babich, S.Y., Glukhov, Y.P., Guz, A.N., (1988), To the solution of the problem of the action of a live load on a two-layer half-space with initial stress, Int. Appl. Mech., 24(8), pp.775-780.
[18] Babich, S.Y., Glukhov, Y.P., Guz, A.N., (2008), Dynamics of a pre-stressed incompressible layered half-space under load, Int. Appl. Mech., 44(3), pp.268-285.
[19] Babich, S.Y., Glukhov, Y.P., Guz, A.N. (2008), A dynamic for a pre-stressed compressible layered half-space under moving load, Int. Appl. Mech., 44(4), pp.388-405.
[20] Demiray, H., (2014), A note on the interactions of nonlinear waves governed by the generalized Boussinesq equation, Appl. Comp. Math., 13(3), pp.376-380.
[21] Dieterman H.A., Metrikine, A.V., (1997), Critical velocities of a harmonic load moving uniformly along an elastic layer, Trans ASME J. Appl. Mech., 64(3), pp.596-600.
[22] Dincsoy, E., Guler, C., Akbarov, S.D., (2009), Dynamical response of a prestrained system comprising a substrate and bond and covering layers to moving load, Mech. Comp. Mater., 45(5), pp.527-536.
[23] Eringen, A.C., Suhubi, E.S., (1975), Elastodynamics, Finite Motion, vol. I; Linear Theory, II, Academic Press, New-York.
[24] Ilhan, N., (2012), The critical speed of a moving time-harmonic load acting on a system consisting a pre-stressed orthotropic covering layer and a pre-stressed half-plane, Appl. Math. Model., 36(8), pp.3663-3672.
[25] Ilyasov, M.X., (2011), Dynamical torsion of viscoelastic cone, TWMS J. Pure Appl. Math., 2(2), pp.203-220.
[26] Jensen, F.B., Kuperman, W.A., Porter, M.B., Schmidt, H., (2011), Computational Ocean Acoustic, 2nd ed. Springer, Berlin, 794p.
[27] Kerr, A.D., (1983), The critical velocity of a load moving on a floating ice plate that is subjected to in-plane forces, Cold. Reg. Sci. Technol., 6(3), pp.267-274.
[28] Metrikine, A.V., Dieterman, H.A., (1999), Lateral vibration of an axially compressed beam on an elastic half-space due to a moving lateral load, Eur. J. Mech. A/Solids, 18, pp.147-158.
[29] Sevdimaliyev, Y.M., Akbarov, S.A., Guliyev, H.H., Yahnioglu, N., (2020), On the natural oscillation of an inhomogeneously pre-stressed multilayered hollow sphere filled with a compressible fluid, Appl. Comput. Math., 19(1), pp.132-146.
[30] Simos, T.E., Tsitouras, Ch., (2020), 6th order Runge-Kutta pairs for scalar autonomous IVP, Appl. Comput. Math., 19(1), pp.392-401.
[31] Sharma, J.R., Kumar, D., (2018), Desing and analysis of a class of weighted - Newton methods with frozen derivative, TWMS J. Pure Appl. Math., 9(2), pp.207-22.
[32] Tsang, L., (1978), Time-harmonic solution of the elastic head wave problem incorporating the influence of Rayleigh poles, J. Acoust. Soc. Am., 65(5), pp.1302-1309.
[33] Zhou, J.X., Deng, Z.C., Hou, X.H., (2008), Critical velocity of sandwich cylindrical shell under moving internal pressure, Appl. Math. Mech., 29(12), pp.1569-1578.

Surkay Akbarov, for a photograph and biography, see TWMS J. Pure Appl. Math., Math., 1(2), 2010, p.154.

Mahir Mehdiyev was born on March 15, 1959 in Azerbaijan. He graduated from Dnepropetrovsk State University (Ukraine), Faculty of Mechanics and Mathematics in 1981. From 1981 to 1983, also from 1988 to 2005 he had been working at the Institute of Mathematics and Mechanics of Azerbaijan National Academy of Science. He received Ph.D. degree in1988 in S.P. Timoshenko Institute of Mechanics of the National Academy of Sciences of Ukraine. From 2005 to the present, he is an associate professor of the Department of Mathematics and Statistics of the Azerbaijan State University of Economics. The topics of his research are the stability and destruction of thin bodies, problems of loss of stability, as well as problems of electrodynamics.

Afig Zeynalov - photograph and biography are absent.